VERIFICATION OF THE SM701 AIRFOIL AERODYNAMIC CHARACTERISTICS UTILIZING THEORETICAL TECHNIQUES

by Kenneth D. Korkan, Robert C. Griffiths and Stefan A. Uellenberg,
Aerospace Engineering Department, Texas A & M University

ABSTRACT

Utilizing a state of the art low speed airfoil design/analysis methodology, the Airfoil Program System (APS) the SM701 laminar flow airfoil was designed specifically for the World Class sailplane by Airfoils, Incorporated. The airfoil was expected to exhibit certain design criteria as predicted by the computational methodology, e.g. docile stall characteristics, high maximum lift with low profile drag and restrained pitching moment. Verification of these characteristics was performed by testing a two-dimensional SM701 airfoil in the Texas A & M University Low Speed Wind Tunnel (TAMU-LSWT) and comparing the theoretical predictions with the experimental results. Comparisons of the results were done implementing graphical output of c_l vs c_d, c_l vs α, and c_m vs α. Further limited comparisons were done with respect to transition location on the airfoil, utilizing flow visualization techniques in the wind tunnel. These transition locations are predicted in the airfoil analysis methodology utilized in this study. The problem of airfoil roughness is also addressed by the (APS). While roughness in the form of grit was not added to the wind tunnel model, predicted theoretical roughness values were included in the test comparisons.

Nomenclature

c	chord length
c_l	lift coefficient
$c_{l_{max}}$	maximum lift coefficient
c_d	drag coefficient

c_m	pitching moment coefficient
$c_{mc/4}$	pitching moment coefficient; quarter-chord
H_n	shape factor
r	roughness factor
p	static pressure
Re	Reynolds number
$u(x,y)$	tangential vel. component in boundary layer
$U(x)$	potential flow velocity
V	velocity
x/c	horizontal airfoil coordinates
x_{cr}/c	critical transition location
y/c	vertical airfoil coordinates
α	angle of attack
$\alpha_{l,o}$	angle of zero lift
$\delta_1(x)$	displacement thickness
$\delta_2(x)$	momentum thickness
$\delta_3(x)$	energy thickness

I. INTRODUCTION

The formulation of an accurate, computational, low speed airfoil analysis methodology has been attempted by theoreticians for more than 30 years. The creation of such an analysis would mean savings in money as well as lives due to the decreased need for extensive flight testing. The first step in determining the validity of such a methodology resides in verification through experimental techniques, such as the use of wind tunnels.

One such methodology that attempts airfoil analysis at low speeds is known as the Airfoil Program System (APS), created by Dr. Richard Eppler of the University of Stuttgart. This approach utilizes a panelling method as well as semi-empirical data and an integral boundary layer method. [1] Upon specification of the airfoil coordinates, Reynolds number and angle of attack, the computer analysis calculates velocity and pressure distributions, lift, drag and moment coefficients, and addresses transition and separation locations. The APS methodology also allows the inclusion of different roughness factors for the airfoil to simulate rain, insects, etc. The system is also capable of designing airfoils for specific purposes, such as the airfoil of interest to this study, designated the SM701.

The SM701 laminar flow airfoil was designed for the World Class sailplane utilizing the APS methodology as developed by Eppler and modified by Mr. Dan Somers of Airfoils, Inc. The design team, consisting of Mr. Somers and Dr. Maughmer of Penn State University, had the goal of achieving specific aerodynamic performance objectives, e.g. high maximum lift and low profile drag with restrained pitching moment in addition to docile stall characteristics.[2]

Verification of the results as predicted by Somers and Maughmer was to be tested by constructing an exact duplicate of the theoretical airfoil, installing the airfoil in the TAMU-LSWT, and testing under the same conditions utilized by Airfoils, Inc. in the APS computer analysis. Due to structural construction limitations, the final airfoil shape was slightly different from the exact SM701, as seen in Figure 1. Important differences were observed between the theoretical SM701 airfoil ("Airfoil 1") and the SM701 airfoil constructed at Texas A & M University ("Airfoil 2").

Airfoil 2 displayed a finite thickness at the trailing edge; Airfoil 1 had a sharp trailing edge. Also, due to some structural differences toward the leading edge, a camber alteration was also expected. The maximum measurable difference between the two airfoils was limited to 0.35%c, according to Nicks.[3] Therefore, to obtain a valid comparison between the experimental and theoretical data, it became necessary to determine the new airfoil coordinates. These coordinates were then used to execute the computational analysis and obtain a valid comparison to the wind tunnel results.

The method utilized to obtain the new airfoil coordinates included cutting a template of the airfoil cross section, followed by a digitizing procedure whereupon the airfoil coordinates were determined by computational methods. These new points were non-dimensionalized, smoothed and re-integrated with the Airfoil Program System. These new results were then compared with the wind tunnel test data to produce a valid comparison.

The aerodynamic coefficients of interest in this study included lift coefficient, drag coefficient, and moment coefficient about the quarter chord. Other characteristics of concern were transition location, maximum lift coefficient, and Reynolds number effects on the coefficients. Special interest was given to differences between the theoretical and experimental results, as well as verifying the desired SM701 airfoil performance objectives.

II. COMPUTATIONAL THEORY

The APS methodology employs the potential-flow analysis method which utilizes panels with distributed surface singularities. The singularities used are parabolically distributed vortices, placed along each panel, and the flow condition requires the tangential velocity component to equal zero along the body surface. The shape of each panel is determined by a polynomial of the third degree, fixed in a local coordinate system. The Kutta condition must also be satisfied at the trailing edge singularity. If the trailing edge has zero thickness, then the airfoil analysis replaces the trailing edge shape with a new one having a zero degree trailing edge, and none of the airfoil coordinates are changed. If the trailing edge has a finite thickness, the APS methodology switches to a different solution which simulates a wake behind the trailing edge.

For the boundary layer calculations, the pressure gradient dp/ds is necessary, where s is the arc length along the airfoil surface. Positive dV/ds means a favorable pressure gradient or negative dp/ds, while a negative dV/ds implies an adverse pressure gradient. An integral method is used for the analysis the boundary layer. If $u(x,y)$ is the tangential velocity component within the boundary layer, then the potential-flow velocity is:

$$U(x) = \lim_{y \to \infty} u(x,y) \tag{1}$$

the displacement thickness is:

$$\delta_1(x) = \int_0^\infty \left(1 - \frac{u(x,y)}{U(x)}\right) dy \tag{2}$$

the momentum thickness is:

$$\delta_2(x) = \int_0^\infty \left(1 - \frac{u(x,y)}{U(x)}\right)\frac{u(x,y)}{U(x)} dy \tag{3}$$

and the energy thickness is:

$$\delta_3(x) = \int_0^\infty \left[1 - \left(\frac{u(x,y)}{U(x)} \right)^2 \right] \frac{u(x,y)}{U(x)} dy \qquad (4)$$

Then the shape factors are taken as:

$$H_{12} = \frac{\delta_1}{\delta_2} \qquad (5)$$

and

$$H_{32} = \frac{\delta_3}{\delta_2} \qquad (6)$$

Approximate solutions can then be determined by allowing only velocity distributions of the form:

$$\frac{u}{U} = f\left(\frac{y}{\delta(x)}, H(x) \right), \qquad (7)$$

where δ is a thickness factor and H a shape factor. Calculations within the analysis are simplified by realizing that H_{32} and δ_2 are functions of H_{12}, δ_1 and δ_3. For values of H_{32} where $1.51509 < H_{32} < 1.57258$, the flow region over the airfoil is assumed to have adverse pressure gradients. These constants are derived in a semi-empirical manner utilizing the so-called Hartree profiles.[1] For turbulent boundary layers, separation is assumed to occur at values of $H_{32} < 1.46$. More generally, boundary layer separation is assumed to occur at a point where $\left(\frac{\partial u}{\partial y} \right)_{y=0} = 0$. This boundary layer process aids in the development of C_{lmax} values, as well as C_l values beyond C_{lmax}. The flowfield analysis utilized in the APS includes results beyond C_{lmax} or effective angle of attack of close to 20 degrees. For a detailed discussion of the APS reference is recommended to Eppler.[1]
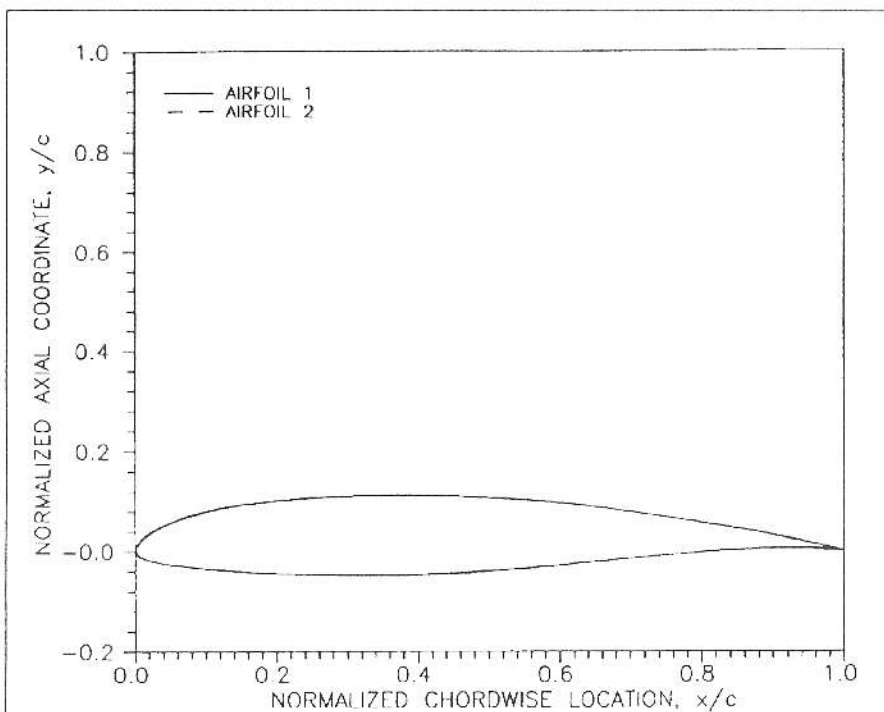
III. METHODOLOGY

The testing of the SM701 airfoil involved an extensive array of parameters necessarily compatible with both the experimental and theoretical investigations. The most important "similarity parameter" was the shape of the airfoil. It was important that the airfoils tested in the tunnel and on the computer were as close to identical as possible, as discussed earlier. A total of five Reynolds numbers were investigated, i.e. 700,000, 1,000,000, 1,500,000, 2,000,000 and 2,500,000. These values fell within the range of capability of the wind tunnel and in the realm of low speed flight for the SM701 airfoil as computationally simulated.

Also, as roughness has a dramatic effect on the performance of a laminar flow airfoil, it was important that the wind tunnel model be as smooth as possible, and since the APS is capable of simulating roughness, choosing the correct roughness factor used in running the methodology was imperative. To show the large difference between a computationally developed smooth and rough airfoil, graphical data will be presented in Section IV. The SM701 wind tunnel model was not roughed during this study, but preliminary results from a separate wind tunnel/computational comparison study display similar trends.[4] The angle of attack values were also important. The range of α values went from beyond negative C_{lmax} through possible C_{lmax}. For the SM701 airfoil, this range was -15° to 18°.

To assess the accuracy of the APS transition prediction, flow visualization techniques were performed on the SM701 airfoil while in the wind tunnel. This included covering a chordwise portion of the airfoil with oil and observing the flow pattern over the wing with ultraviolet, or "black" lights. The transition point was not difficult to determine from this method. Separation conditions, especially laminar separation bubbles, were also examined during this flow visualization process. However, owing to the time consuming nature of this experimental methodology, only a limited number of flow visualization tests were conducted.

In summary, two different disciplines were active during this study, i.e. those of the experimentalists and the theorists. The experimentalists concentrated on constructing an accurate wind tunnel model and conducting tests in an environment as free from anomalies as possible. They were also responsible for correcting any errors found during the tests. The theoreticians, however, were responsible for recreating a physical environment in a computational methodology. The merging of the two philosophies always produces interesting results.

IV. RESULTS

The aerodynamic coefficients obtained from the APS analysis were compared to the experimental data resulting from wind tunnel research on the SM701 airfoil.[3] Implementing the corrected airfoil coordinates with the com-

FIGURE 1. Comparison of the designed and actual constructed SM-701 airfoil. See Figure 3. for a larger version of this diagram.
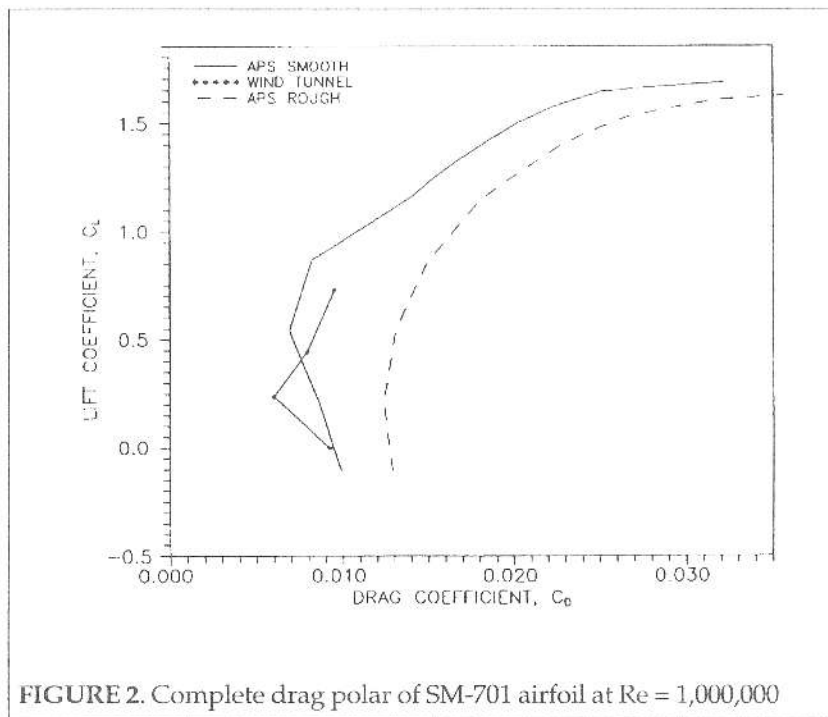
FIGURE 2. Complete drag polar of SM-701 airfoil at Re = 1,000,000

puter methodology, similar results were expected between the theoretical and experimental studies of the SM701 airfoil.

Drag Polar

The APS was consistent in predicting a lower drag coefficient value at higher lift coefficients than that shown from the wind tunnel data (momentum loss measurements). At the same time, the wind tunnel results showed lower c_d's at smaller values of c_l. In other words, the laminar "bucket region," the area of concern for the World Class sailplane, was shifted "downwards" for the wind tunnel data. Figure 2, which displays the drag polar for a Re of 1,000,000, shows this trend for the entire range of Reynolds numbers. Also displayed is the roughed APS results. As expected for the roughed data, the drag coefficient increased and can be seen in Figure 2. Here, in the laminar bucket region where $c_l = 0.4$, the predicted c_d values nearly double between the smooth and rough results. As Re increases to 1,500,000 and 2,500,000 as seen in Figures 3 and 4 respectively, a decrease in c_d is apparent. This was expected as an increased Re value tends to increase the turbulence of the flow over an airfoil, resulting in the flow field staying attached to a further aft chordwise location postponing separation. In all five Reynolds number tests, the trends displayed in Figures 2, 3 and 4 are similar. The wind tunnel results fall between the smooth and rough values as predicted by the APS analysis.

The accuracy of the design criterion can be deduced from these three Figures also. According to the designers of the SM701, the c_{lmax} of at least 1.6 should occur at a c_d value of approximately 0.0240. However, both the theoretical and experimental curves display docile stall characteristics as evidenced by the gentle curve in the c_{lmax} region.

Lift Coefficient vs. Angle of Attack

As shown in Figures 5, 6 and 7, the α_{l_o} point has shifted between the theoretical and experimental results. The shift is approximately one half degree to the positive side for the wind tunnel results. However, the lift curve slope ($\frac{d_l}{d\alpha}$) is the same for both. The maximum lift coefficient as predicted by the APS was determined from a set of boundary conditions developed empirically by Somers and Maughmer. The c_{lmax} was considered to have occurred when either the c_d value of the upper surface exceeded 0.024 or if the length of turbulent separation along the upper surface increased beyond the 0.1c location, as measured from the trailing edge. On Figure 5, the c_{lmax} value for the wind tunnel model was shown to be lower than the smooth theoretical, e.g., from 1.561 to 1.5122. The α's at which c_{lmax} occurs in each case are consistent; approximately 11° for the APS calculations and 15° for the wind tunnel results, as displayed in Figures 5-7. Again on Figure 5, the negative c_{lmax} values correspond closely, occurring near -10° with a c_l value close to -0.5. Also in Figures 5, 6 and 7, the theoretical with roughness results are also included for comparison analysis. Generally, as shown in all three c_l vs α figures, the only variation from the APS determined values for the smooth and rough data occurred around the positive and negative c_{lmax} values.

As the Reynolds number increases to 1.5 million (Figure 6) and to 2.5 million (Figure 7) certain trends become apparent. First, the c_{lmax} values predicted by APS for the smooth airfoil increases from close to 1.7 to near 1.84. The positive c_{lmax} value for the wind tunnel model remained
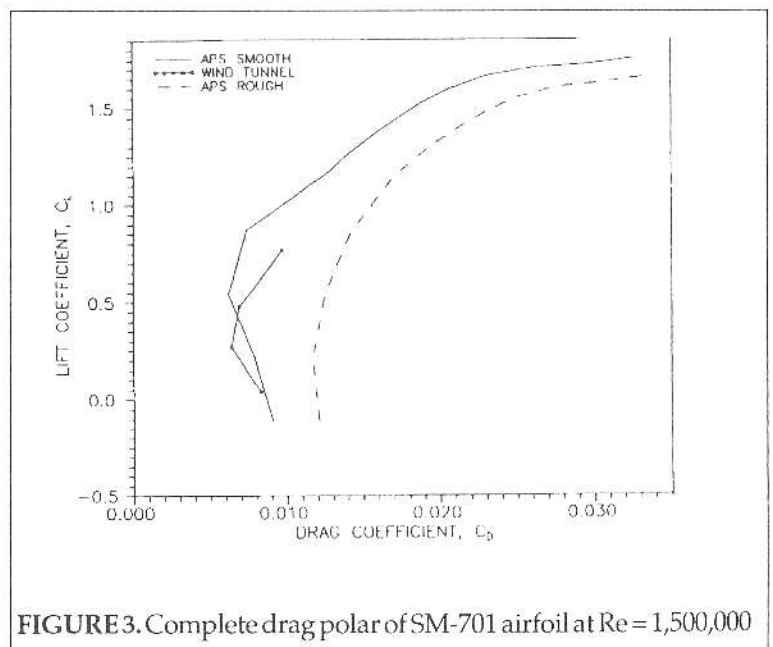

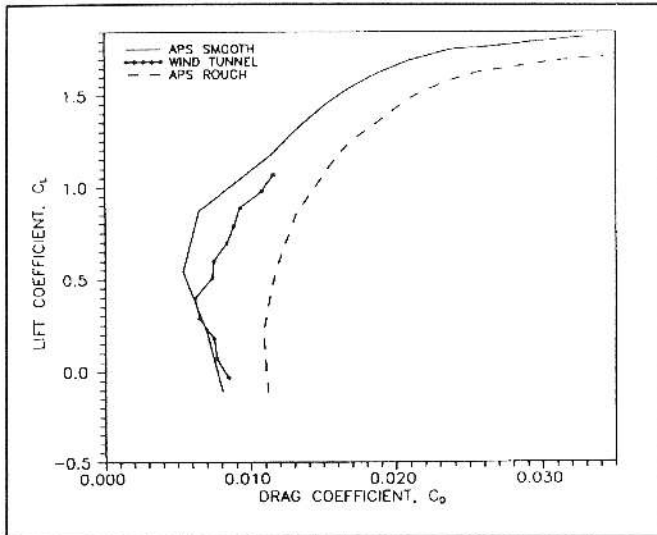**FIGURE 3.** Complete drag polar of SM-701 airfoil at Re = 1,500,000

FIGURE 4. Complete drag polar of SM-701 at Re = 2,500,000

FIGURE 5. Comparison of APS methodology to wind tunnel results of the SM-701 airfoil at Re - 700,000

FIGURE 6. Comparison of APS methodology to wind tunnel results of the SM-701 airfoil at Re = 1,500,000
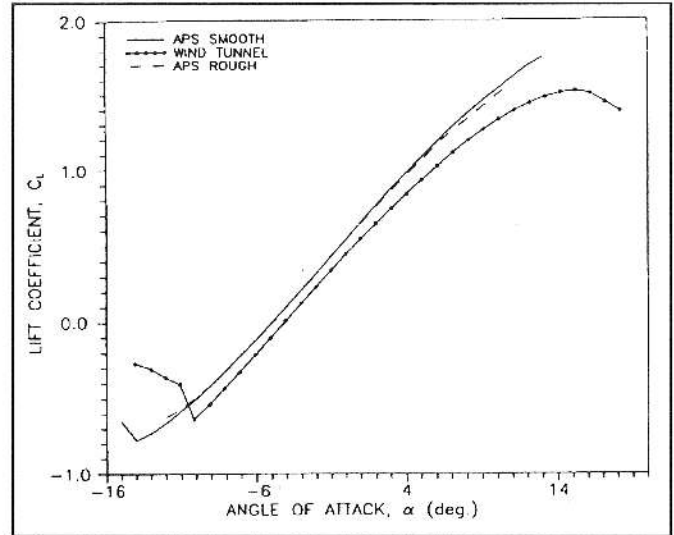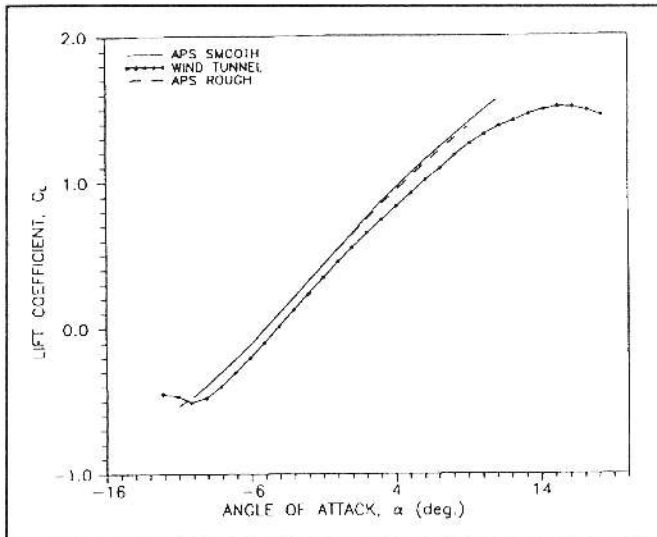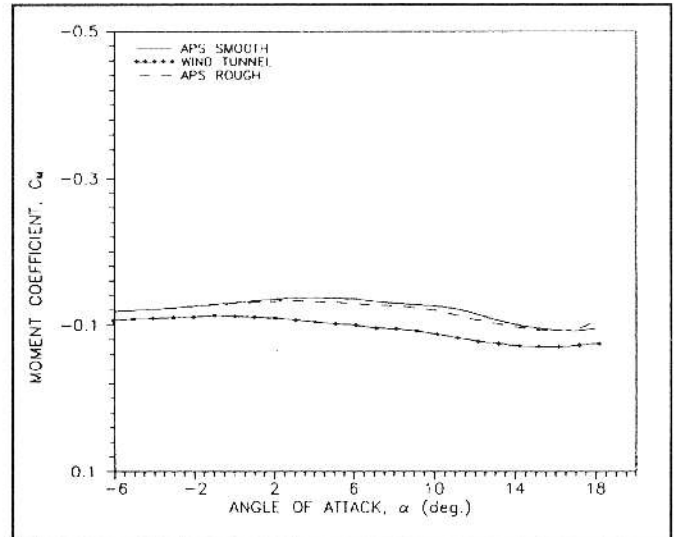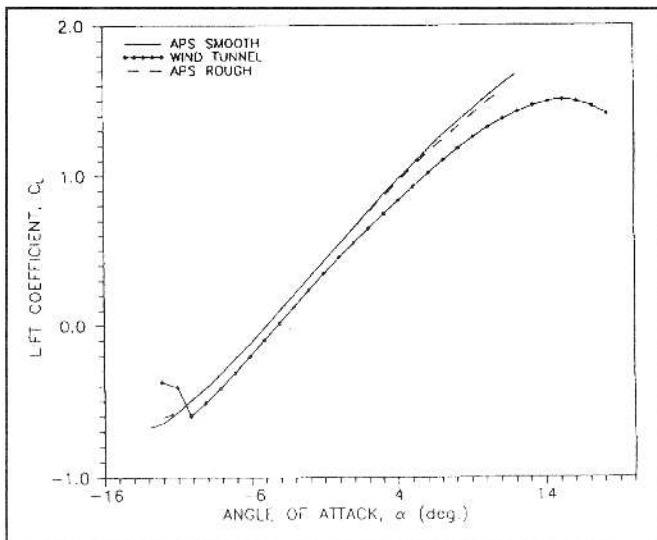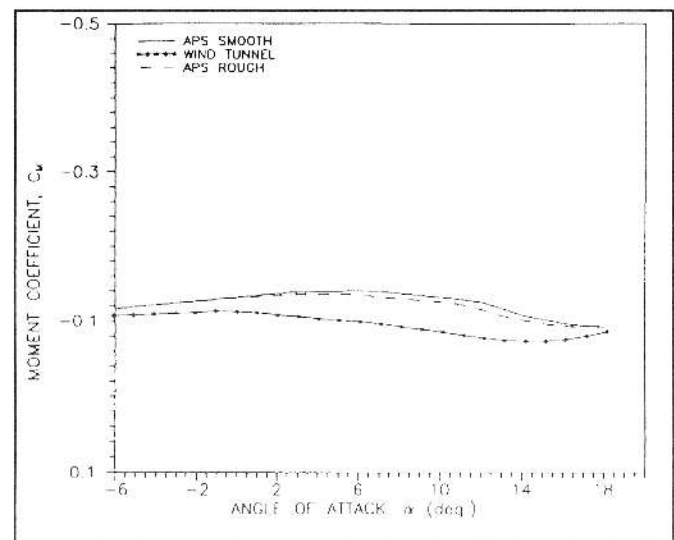

FIGURE 7. Comparison of APS methodology to wind tunnel results of the SM-701 airfoil at Re = 2,500,000

FIGURE 8. Comparison of APS methodology to wind tunnel results of the SM-701 airfoil at Re = 700,000

FIGURE 9. Comparison of APS methodology to wind tunnel results of the SM-701 airfoil at Re = 1,500,000
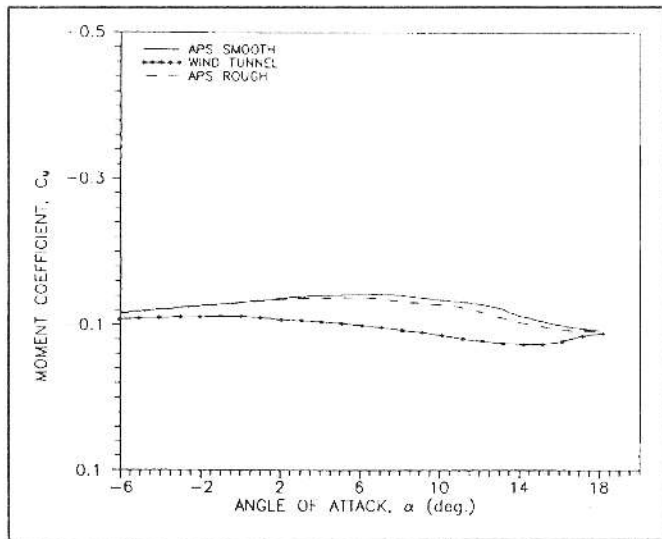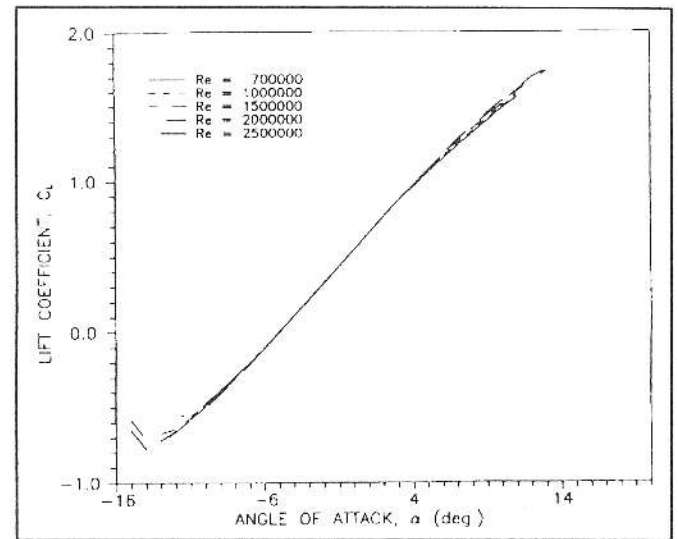
FIGURE 10. Comparison of APS methodology to wind tunnel results of the SM-701 airfoil at Re = 2,500,000

FIGURE 13. Theoretically acquired lift characteristics of the msmooth SM-701 airfoil at various Reynolds numbers.
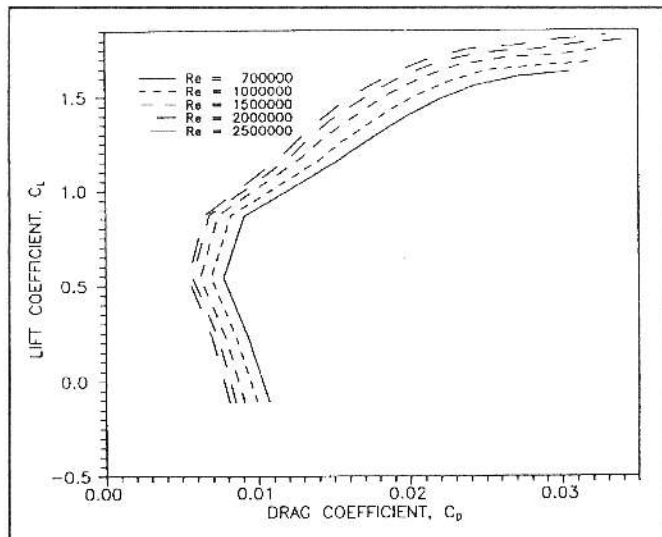

FIGURE 11. Theoretically acquired drag polars smooth SM-701 airfoil at various Reynolds numbers.
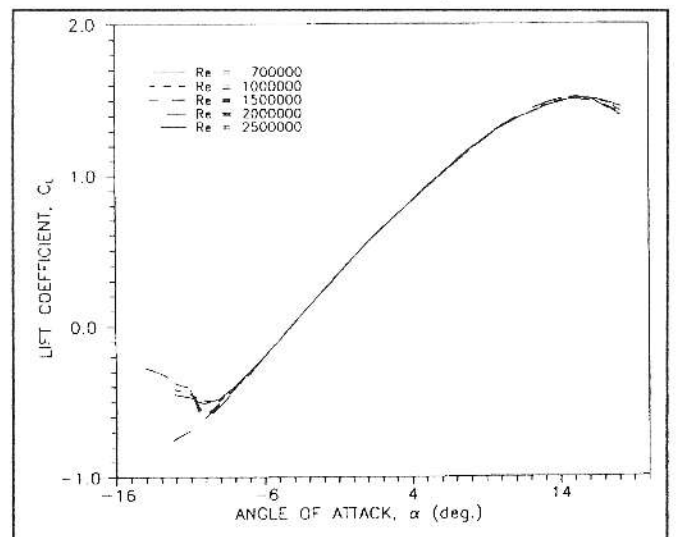

FIGURE 14. Experimentally acquired lift characteristics of the smooth SM-701 airfoil at various Reynolds numbers.
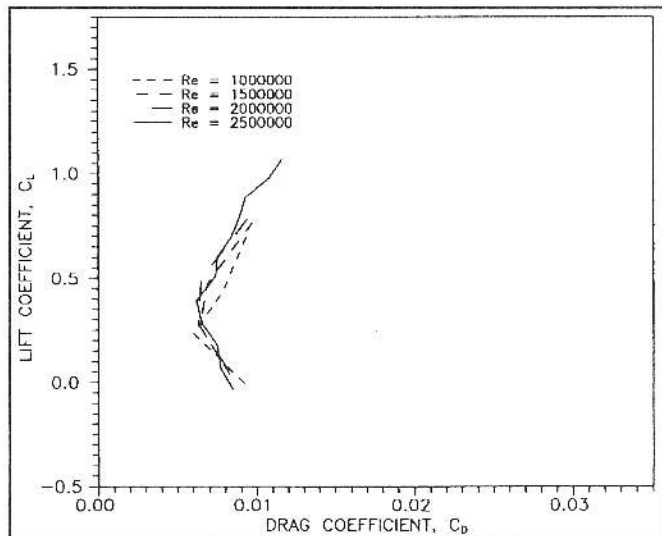

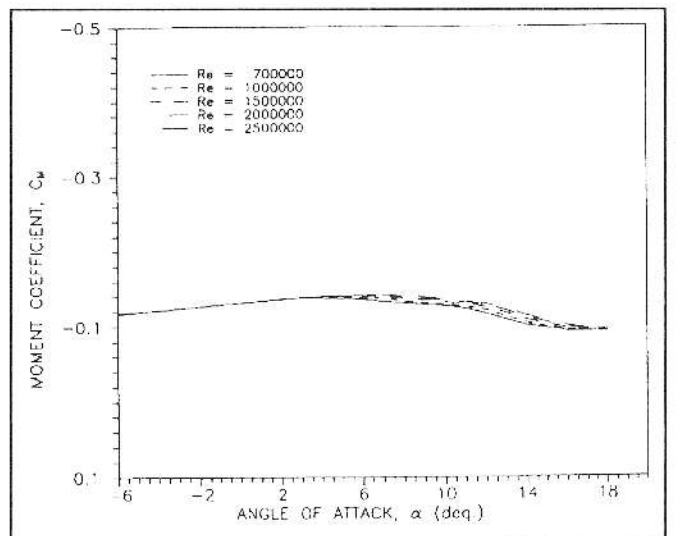**FIGURE 12.** Experimentally acquired drag polars of the SM-701 airfoil at various Reynolds numbers.

FIGURE 15. Theoretically acquired moment characteristics of the smooth SM-701 airfoil at various Reynolds numbers.
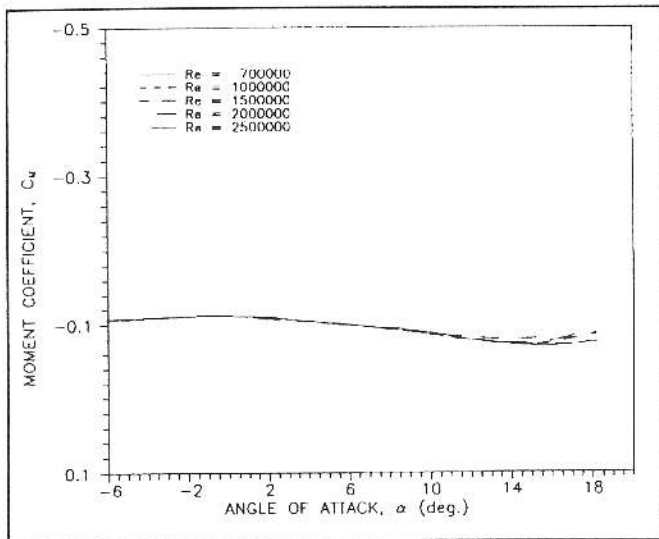
FIGURE 16. Wind tunnel acquired moment characteristics of the smooth SM-701 airfoil at various Reynolds numbers.
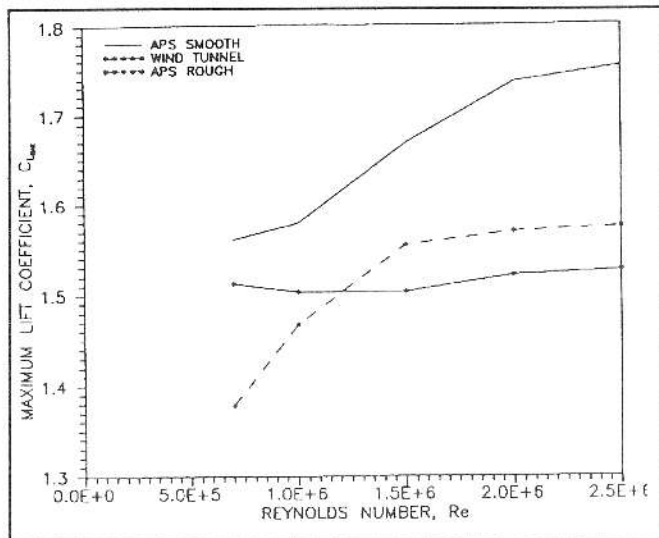

FIGURE 17, Comparison of Reynolds number effect on the maximum lift coefficient of the SM-701 airfoil.
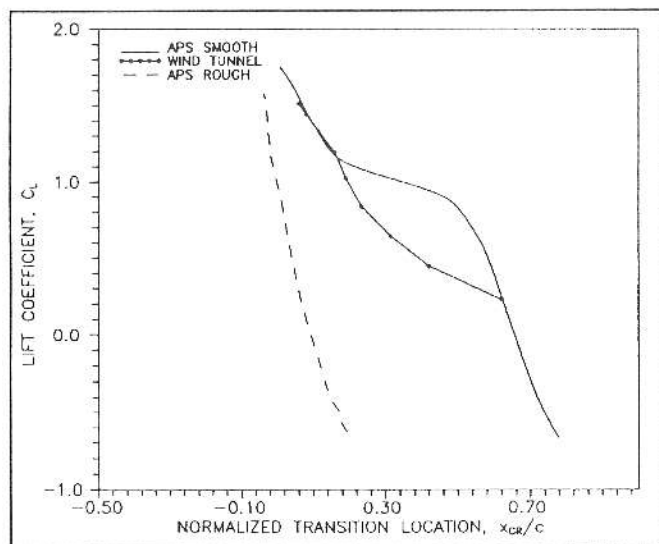

FIGURE 18. Comparison of transition location on the upper surface of the SM-701 airfoil at Re = 2,500,000

virtually identical. The wind tunnel model did display slightly less docile stall characteristics beyond c_{lmax} for increasing Re. Negative c_{lmax} was shown to exhibit more negative values for increasing Re, as shown again in Figures 5,6 and 7. This trend occurred for both the theoretical and the experimental airfoils. However, while the angle at which negative c_{lmax} occurred for the wind tunnel model remained close to -10° negative c_{lmax} for the theoretical airfoil occurred at increasingly negative a values as Re increased ranging from -10° in Figure 5 to -14° in Figure 7. The rough values showed more intolerance to changing Re, remaining between -11° and -12° for all five Reynolds numbers.

Pitching Moment Coefficient vs. Angle of Attack

The $c_{mc/4}$ vs α values showed an insensitivity to changing Reynolds numbers, as shown in Figures 8,9 and 10. The smooth and rough theoretical values remained very close to each other, never varying by more than 2.5%. The difference between the theoretical and experimental values is larger, but remained constant throughout the range of Reynolds numbers tested. The trends displayed between the theoretical and experimental c_m are similar, however, as shown in the c_m vs α Figures. Both the wind tunnel model and the theoretical airfoil display c_m values in excess of -0.1, which is the design criterion specified for the SM701 airfoil. However, the theoretical model at no time, for the five Reynolds numbers tested, exceeded -0.148, while the experimental model never exceeded -0.12. Therefore, the restrained moment criterion was met under both conditions, even though values greater than -0.1 were reached. It was found that the design of the SM701 airfoil with 16 percent thickness and a c_{lmax} of at least 1.6 with acceptably low profile drag coefficients could not be achieved without violating the -0.1 pitching moment coefficient constraint.[2]

Reynolds Number Effect

There was a Reynolds number effect on the results of this study. As shown in Figure 11, the theoretically acquired drag polar displays a decreasing c_d value for increasing Re. The same trend is displayed in Figure 12 for the wind tunnel tests. Reynolds number effect on lift was negligible except near positive c_{lmax} and negative c_{lmax}, as shown in Figures 13 and 14 for theoretical and experimental results of c_l vs α data. The moment coefficient characteristics were shown to be little affected by changing Re, especially at negative and small positive α's. This is shown in Figure 15 for the theoretical airfoil and in Figure 16 for the experimental SM701. Angles of attack above 5 degrees display a slight influence of Reynolds number. Figure 17 shows the effect Re had on c_{lmax} values. The wind tunnel data show little effect, while the roughed theoretical values display an increase in c_{lmax} with an increase in Re. The smooth data show an even greater change with increasing Reynolds number.

Transition

The flow visualization technique employed on the SM701 airfoil was successful in showing transition location over the airfoil at different angles of attack. However, due to time constraints, data were only compiled on a single Reynolds number run, which included an angle sweep from -2° to 18°. Increasingly negative angles of attack were

unnecessary as the upper surface of the wing was observed, not the lower. Also, the upper surface at positive angles of attack is the more realistic flight profile for a sailplane, especially during a landing approach. At the higher angles of attack, stall characteristics could be observed on the upper surface of the wing, in particular transition and separation. The experimental transition locations observed at a Reynolds number of 2,500,000 were compared to those predicted by the Airfoil Program System as shown in Figure 18. This figure shows transition location from the leading edge of the airfoil in percent chord versus lift coefficient at a constant Re of 2,500,000. The "rough" results show transition occurring the closest to the leading edge of the airfoil, as can be expected. The experimental results diverge from the theoretical "smooth" data at approximately 20% from the leading edge location, reconverging at close to the 65% position. This divergence could correspond to a premature tripping of the boundary layer on the wind tunnel model due to roughness, or an inadequacy in the APS analysis. This difference is most pronounced in the c_l of 0.6 region.

The presence of laminar separation bubbles was impossible to confirm on the airfoil. The importance of laminar separation bubbles cannot be ignored as when they occur, a tremendous amount of drag appears on the wing. Failure to include the effects of these bubbles in drag calculations will cause an underprediction of the c_d value. The inability to confirm the presence of the laminar separation bubbles could be due to experimental technique and the fact that the bubbles were too short to be positively observed with the human eye.

V. CONCLUSIONS

Verification of the APS by experimental methods proved to be largely successful. Theoretical values of c_l, c_{lmax} and $c_{mc/4}$ matched the experimental values and trends. The values predicted for c_d tended to be less than the experimental values for the "smooth" SM701 airfoil, often by a factor of two or more. This could be attributed to the failure of the APS to predict proper transition and separation locations consistently. The failure to predict any laminar separation bubbles on the upper or lower surfaces under actual flight or wind tunnel experimentation is probably not realistic, therefore resulting in an underprediction of drag coefficient.

The docile stall characteristics exhibited by the airfoil near clmax could be attributable to the elimination of large laminar separation bubbles on the upper surface. This would also explain their absence during the flow visualization experiments. A docile stall was exhibited in both the theoretical and the experimental results. Low drag was experienced by both airfoils, i.e., c_d was close to the design requirement of 0.024 at c_{lmax}. The maximum lift coefficient was satisfied for the APS predictions, but underpredicted by the wind tunnel experiments. Restrained pitching moment characteristics were shown to occur during both experiments. Not surprisingly, the APS predictions are closer to the airfoil design specifications than the wind tunnel results.

A cause for discrepancy between the experimental and theoretical values would lie in the impossibility of producing the exact coordinates of the slightly modified experimental airfoil for theoretical experimentation. Any difference between the coordinate date sets would cause varying results. Boundary layer effects from the walls of the wind tunnel, a floor "suction" and three-dimensional effects caused by gaps in the test section floor and ceiling, and other experimental anomalies would also create random differences in the test results. Even with the errors and discrepancies, the overall results suggest great promise with the APS as a valid low speed airfoil analysis system.

VI. ACKNOWLEDGMENTS

REFERENCES

1. Eppler, R. "Airfoil Program System. User's Guide." R. Eppler, c. 1990.
2. Somers, D.M. and Maughmer, M.D. "The SM701 Airfoil," Airfoils, Inc, December 1990. Technical Soaring Vol. 16, No.
3. Nicks, O., Steen, G., Heffner, M. and Bauer, D. "Wind Tunnel Investigation and Analysis of the SM701 Airfoil." Technical Soaring, Vol 16, No. **
4. Griffiths, R.C. "Study of Theoretical and Wind Tunnel Results on Flight Performance Degradation due to Ice Accretion."
5. Abbott, I.H. and Von Doenhoff, A.E., "Theory of Wing Sections, Dover Publications, New York, 1959.
6. Schlichting, H., Boundary Layer Theory. McGraw-Hill Book Company, New York, 1979.